

NEW HIGH PROPER MOTION STARS FROM THE DIGITIZED SKY SURVEY. III. STARS WITH PROPER MOTIONS $0.45 < \mu < 2.0'' \text{YR}^{-1}$ SOUTH OF DECL. $=-30^\circ$.¹

SÉBASTIEN LÉPINE

Department of Astrophysics, Division of Physical Sciences, American Museum of Natural History, Central Park West at 79th Street, New York, NY 10024,
USA

Accepted by the Astronomical Journal

ABSTRACT

We report the discovery of 182 new southern stars with proper motion larger than $0.45'' \text{yr}^{-1}$. The stars were found in an expansion of the SUPERBLINK proper motion survey to 8980 square degrees south of Decl. $=-30^\circ$. The new high proper motion stars include 123 objects with $\mu > 0.5'' \text{yr}^{-1}$, and 5 with $\mu > 1.0'' \text{yr}^{-1}$. These new stars consist in a variety of nearby red dwarfs and white dwarfs, and (slightly more distant) red halo subdwarf, and are all prime targets for follow-up spectroscopic and astrometric (parallax) observations. Comparison with previous proper motion surveys in the southern sky suggests that SUPERBLINK has a recovery rate between 80% and 90% at southern declinations for stars with red magnitude $10 < R_F < 19$ and proper motion in the range $0.5 < \mu < 2.0'' \text{yr}^{-1}$. This survey makes a significant addition to the census of high proper motion stars at southern declinations.

Subject headings: astrometry — surveys — stars: kinematics — solar neighborhood

1. INTRODUCTION

Surveys of stars with large proper motions are very effective in identifying low-luminosity objects in the vicinity of the Sun. Most of the white dwarfs and red dwarfs in the Solar neighborhood have first been discovered in proper motion surveys. Much of the current census of nearby stars is based on follow-up analysis of objects listed in large catalogs of high proper motion stars, most notably the NLTT catalog of stars with $\mu > 0.18'' \text{yr}^{-1}$ Luyten (1979b) and (especially) its subset, the LHS catalog of stars with $\mu > 0.5'' \text{yr}^{-1}$ Luyten (1979a). Objects with annual proper motions in excess of $\mu = 0.5''$ are now often referred to as “LHS stars”. The current census of nearby stars is largely based on follow-up observations of those Luyten objects (Gliese & Jahreiss 1991; Gizis & Reid 1997; Reid *et al.* 2003).

The Luyten catalogs have long been known (Dawson 1986) to suffer from significant incompleteness both at low Galactic latitudes ($|b| < 10$), and in southernmost declinations (Decl. $< -32^\circ$). The desire to build a complete census of stars in the Neighborhood of the Sun has motivated a series of new proper motion surveys which, over the years, have gradually filled up these gaps. Recently, improved data-mining techniques have been used to conduct a massive proper motion survey of the northern sky, using data from the Digitized Sky Survey (DSS). In a systematic analysis of DSS scans with the SUPERBLINK software, an automated blink comparator, several hundred new $\mu > 0.5'' \text{yr}^{-1}$ stars have been discovered in the northern sky, effectively filling up the low Galactic latitude gap (Lépine, Shara, & Rich 2002), and also significantly increasing the completeness of the proper motion census at high Galactic latitude (Lépine, Shara, & Rich 2003). In fact, the new *LSPM-north catalog* of stars with proper motions $\mu > 0.15'' \text{yr}^{-1}$ (Lépine & Shara 2005), which compiles the SUPERBLINK results, is now superseding the Luyten catalogs for all areas north of the celestial equator.

The southern sky has been very attractive for proper mo-

tion hunters in recent years, because of the low completeness of the LHS catalog at southern declinations. Several small proper motion surveys have been carried, including the CalánESO (CE) Proper Motion Survey (Ruiz *et al.* 2001), the WT survey (Wroblewski & Torres 1997; Wroblewski & Costa 2001), and the APMPM survey (Scholz *et al.* 2000), which have all made significant additions to the zoo of $\mu > 0.5'' \text{yr}^{-1}$ proper motion stars, although limited in area. Two larger proper motion surveys have recently been conducted based on data from the SuperCOSMOS Sky Survey (SSS). The Liverpool-Edinburgh high proper motion (LEHPM) survey (Pokorny, Jones, & Hambly 2003) has covered $\approx 7,000$ square degrees of the south Galactic cap, including a large fraction of the largely incomplete Decl. $< -32^\circ$ cap. The SuperCOSMOS-RECONS survey (SCR) now aims to obtain an improved proper motion survey of the entire southern sky, although results have so far been presented for $\approx 5,000$ sq.deg. south of Decl. $< -47^\circ$ (Subasavage, *et al.* 2005).

Encouraged by the impressive results already obtained with SUPERBLINK in the northern sky, I have now expanded the analysis of DSS images to the southern declinations. In this paper, I report the discovery of a first set of 182 new stars with $\mu > 0.45'' \text{yr}^{-1}$, found after completing the analysis of 87.1% of the sky south of Decl. $< -30^\circ$ (8980 square degrees). The search methodology is outlined in §2. Results are described in §3. The completeness of our survey is estimated in §4. Finder charts for all new objects are provided in the appendix.

2. SEARCH AND IDENTIFICATION

Our method for identifying high proper motion stars from the Digitized Sky Survey (DSS) is described in much detail in Lépine & Shara (2005). Scans from the DSS are analyzed using SUPERBLINK. For each detection, SUPERBLINK generates two-epoch finding charts which are blinked on the computer screen and examined by eye, in order to filter out any false detection. The whole northern sky has already been analyzed with SUPERBLINK, and the first major data release can be found in Lépine & Shara (2005).

Analysis of the southern declinations of the DSS by SUPERBLINK presents an additional complication. In the northern hemisphere, the DSS incorporates scans from photo-

¹ Based on data mining of the Digitized Sky Survey, developed and operated by the Catalogs and Surveys Branch of the Space Telescope Science Institute, Baltimore, USA.

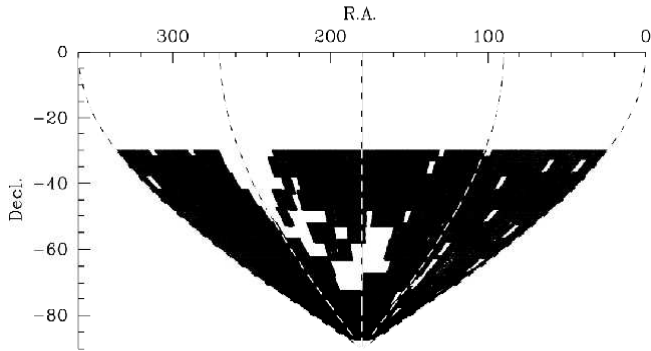


FIG. 1.— Area currently covered in our southern sky proper motion survey (shaded in black). The survey covers 8,980 square degrees, or 87.1% of the sky south of Decl. $=-30^\circ$. Several areas are excluded from the survey because the DSS does not have a suitable first epoch (in particular: several low Galactic latitude plates). Other areas are excluded because the temporal baseline between the first and second epoch images is too short.

graphic plates in the red passband at both the first (POSS-I red; 103aE emulsion) and second epoch (POSS-II red; IIIaF emulsion). In the south, however, the DSS only contains first epoch blue plate (SERC-J blue; IIIaJ emulsion) while the second epoch images are available only from red (SES red; IIIaF emulsion) and far red plates (IVn emulsion). This is problematic, because SUPERBLINK is based on image subtraction algorithms, and thus works best on pairs of images that are as similar as possible. Nevertheless, tests have shown the procedure to work reasonably well on pairs of images in different passbands, as long as there is a sufficient number of stars with similar plate intensities on both images. Tests have shown that SUPERBLINK can recover high proper motion stars from pairs of blue/red plates, although it fails to detect objects with extreme colors. Encouraged by these results, it has been decided to expand the SUPERBLINK analysis of the DSS to southern declinations. The analysis of areas south of Decl. $=-30^\circ$ has now already been completed.

Not all areas of the DSS are suitable for analysis by SUPERBLINK, however. There are several zones where first epoch SERC-J plates are unavailable, most notably at low Galactic latitudes. Proper motion searches also require that there be a sufficient temporal baseline between the first and second epoch. This was rather apparent in the northern sky, where the POSS-I plates precede the POSS-II plates by ≈ 40 years. But in the southern sky, the baseline between the SERC and SES surveys is significantly shorter (< 20 years). In some cases, the baseline is too short for accurate proper motion detection/measurement. Pairs of plates with baselines under 5 years were thus not considered for our analysis. The SUPERBLINK algorithms also fail in subfields ($17' \times 17'$) where there is an extended, saturated object, such as very bright $V < 5$ star. In the end, 8980 square degrees, or $\approx 87.1\%$ of the sky south of Decl. $=-30^\circ$, were successfully analyzed (Figure 1).

DSS scans were provided as input to the SUPERBLINK software. Lists of candidate high proper motion stars were generated on output, along with the usual $4.25' \times 4.25'$ finder charts. The charts were visually examined by blinking on a computer screen, and bogus detections were filtered out. Counterparts for all confirmed objects were searched for in the *USNO-B1.0 catalog* (Monet *et al.*

2003) and in the *2MASS All-sky Catalog of Point Sources* (Cutri *et al.* 2003). The 2MASS positions were used as a reference to calculate the 2000.0 epoch position. Optical magnitudes were obtained from USNO-B1.0, infrared magnitudes from 2MASS.

3. HIGH PROPER MOTION DISCOVERIES

A total of 1,147 stars with proper motions in the range $0.45 < \mu < 2.0'' \text{ yr}^{-1}$ were located by SUPERBLINK. A majority of these have been previously reported in the literature as high proper motion stars. The list of SUPERBLINK detections was cross-correlated with the NLTT catalog, and with lists of detections from the APMPM survey (Scholz *et al.* 2000), the CE survey (Ruiz *et al.* 2001), the LEHPM catalog (Pokorny, Jones, & Hambly 2003), and the recent SCR proper motion survey (Subasavage, *et al.* 2005). A search was also made with Simbad², to identify known high proper motion stars from other sources, especially the WT stars (Wroblewski & Torres 1997; Wroblewski & Costa 2001). In all, 965 of the SUPERBLINK detections were found to be known high proper motion stars.

A total of 182 new high proper motion stars were discovered with SUPERBLINK. A complete list is presented in Table 1. Names for the stars are based on the convention introduced by Eggen (1979, 1980). We use the letters “PM” for *Proper Motion*, followed by a space, followed by the letter “J” which denotes that the following digits refer to the J2000 coordinates. The numerals then correspond to the right ascension (to 0.1 minutes of time) and declination (to 1 minute of arc). In case of confusion between two objects, most notably close proper motion doubles, we add the directional suffix “N”, “S”, “W”, or “E” to distinguish between the two components.

Finder charts for all the stars can be found in the appendix. Stars range in magnitude from $R_F = 11.3$ to $R_F = 20.5$. Most notably, the list includes 5 new stars with proper motions exceeding $1.0'' \text{ yr}^{-1}$. These are PM J00522-6201, LPM J12277-4541, LPM J13384-3752, LPM J19167-3638, and LPM J19261-4310. The list also includes two common proper motion doubles: LPM J19105-4132 / LPM J19105-4133, and LPM J22403-4931E / LPM J22403-4931W.

Figure 2 plots the distribution on the sky of all the stars found with SUPERBLINK, with new discoveries denoted by larger symbols. New stars are found all over the survey area, although relatively fewer ones are found near the south Galactic cap (an area covered by the LEHPM catalog), and in areas south of Decl. $=-47^\circ$ (where the SCR survey has already made an efficient pass).

Table 1 provides J2000 coordinates for the stars at the 2000.0 epoch. The temporal baseline between the first and second epoch of the discovery plates is given. The measured proper motions are *relative*, calculated with respect to background Galactic stars. Proper motion errors (μ_{err}) are estimated based on the detailed analysis of SUPERBLINK errors from Lépine & Shara (2005), with normalization to the temporal baseline (a shorter baseline makes the proper motion less accurate). Optical magnitudes B_J , R_F , and I_N (respectively photographic IIIa-J, IIIa-F, and IV-N) are listed; these are obtained from counterparts of the stars found in the USNO-B1.0 catalog (Monet *et al.* 2003). Infrared J, H, and K_s magnitudes are also given for stars that have counterparts in the 2MASS All-Sky Catalog of Point Sources (Cutri *et al.*

² <http://simbad.u-strasbg.fr/>

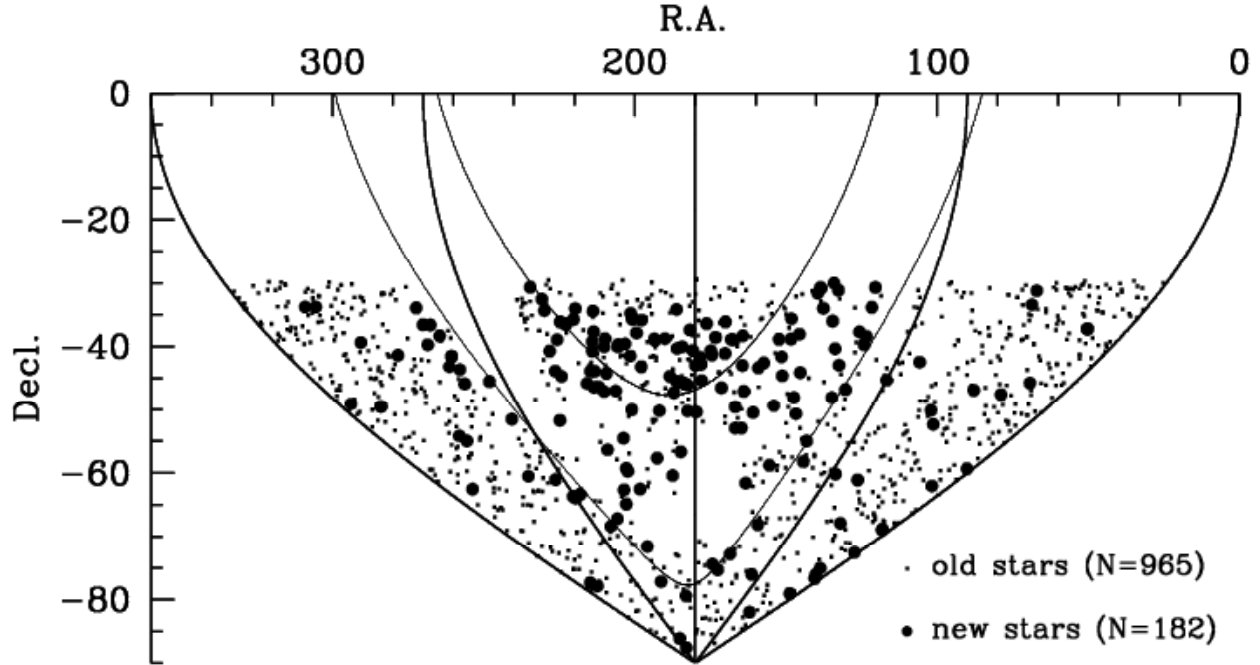


FIG. 2.— Objects with $\mu > 0.45''$ found in the survey area with SUPERBLINK. The software correctly re-identified a total of 965 previously known high proper motion objects (“old stars”). SUPERBLINK also discovered 182 new high proper motion objects (“new stars”), which are here reported as high proper motion stars for the first time.

2003).

A simple reduced proper motion analysis provides an estimate of the spectral class of the stars. Optical to infrared proper motion diagrams (Salim & Gould 2002) can be used to separate faint high proper motion stars into three general classes: white dwarfs (wd), subdwarfs (sd), and disk dwarfs (d). Here we use a $[H_{R_F}, R_F - K_s]$ reduced proper motion diagram and relationships defined in Lépine, Rich, & Shara (2003), where $H_{R_F} = R_F + 5 \log(\mu) + 5$. Figure 3 shows the distribution, in the reduced proper motion diagram, of all 1,147 stars found by SUPERBLINK, with the new discoveries again labeled with larger symbols. Among the new discoveries, there are 14 candidate white dwarfs, 52 candidate halo subdwarfs, and 106 candidate disk dwarfs. The status of nine other stars remains ambiguous because of incomplete photometric information.

4. COMPLETENESS OF SUPERBLINK IN THE SOUTHERN SKY

To estimate the completeness of our survey, we have compared our list of SUPERBLINK detections to lists of high proper motion stars from five previous southern surveys which overlap with our search areas. Within the 8980 square degrees area analyzed with SUPERBLINK, we compiled a total 769 stars with magnitude $10 < R_F < 19$ and proper motion with $0.5 < \mu < 2.0''$ from the NLTT catalog (Luyten 1979b), the APMPM survey (Scholz *et al.* 2000), the CE survey (Ruiz *et al.* 2001), the LEHPM catalog (Pokorny, Jones, & Hambly 2003), and the SCR survey (Subasavage, *et al.* 2005). Note that stars brighter than magnitude $R_F \approx 10$ are generally not recovered by SUPERBLINK because they form extended saturated patches on the SERC-J and SES plates; these are thus excluded from the completeness analysis. Proper motions for all those bright stars can be obtained from the TYCHO-2 catalog (Hog *et al.* 2000). From

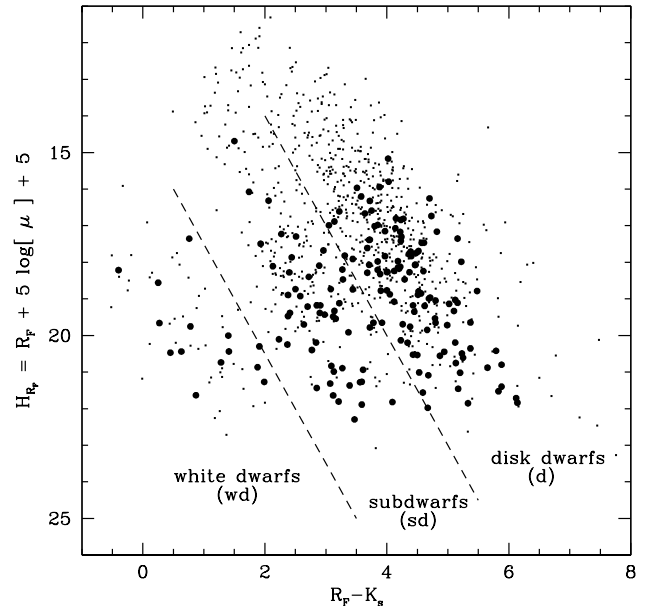


FIG. 3.— Reduced proper motion diagram of the high proper motion stars identified with SUPERBLINK. Small circles denote previously known objects, and large circles denote new discoveries, as in Figure 2. The approximate loci of white dwarfs, halo subdwarfs, and disk dwarfs are indicated, as from Lépine, Shara, & Rich (2002). The new SUPERBLINK stars tend to be relatively faint ($R_F > 14$) and so populate mostly the lower half of the diagrams, where low-luminosity objects normally lie (white dwarfs, low-mass dwarfs and subdwarfs). The new stars make a significant addition to the census of objects with $H_{R_F} > 20$.

the reference sample of fainter ($R_F > 10$) stars SUPERBLINK recovered 612 objects, missing 157, suggesting recovery rate of 79.5%.

It must be noted, however, that NLTT catalog entries are sometimes affected by large positional errors (Salim & Gould 2003). It is thus very possible that a number of NLTT objects have been “missed” by SUPERBLINK simply because they do not exist at the position recorded in the NLTT catalog. Likewise, Subasavage, *et al.* (2005) report problems recovering some the stars listed in the LEHPM catalog; it appears that a number of LEHPM entries are either spurious, or have large errors in their reported position. Further investigations would be required to determine which of the NLTT and/or LEHPM objects are not real. In any case, the SUPERBLINK recovery rate quoted above is probably an underestimate. In fact, if we exclude from the analysis stars all the stars that are listed only in the NLTT or LEHPM, we reduce the reference sample to 259 previously known stars in our survey area, of which only 26 have been missed by SUPERBLINK. This suggests a higher recovery rate of $\approx 90\%$. The actual recovery rate of SUPERBLINK most probably lies somewhere between these two estimates.

In any case, it appears that the SUPERBLINK recovery rate in the south is significantly lower than the much superior detection rate ($\approx 99\%$) achieved at northern declinations (Lépine & Shara 2005). The lower efficiency of SUPERBLINK in the southern sky is most likely due to the fact that plates of different colors (blue/red) are used for the first and second epoch. Because SUPERBLINK is an image-subtraction analysis software, more confusion arises when plates of different passbands are compared. In particular, one of our algorithms for the identification of moving objects requires that they display similar intensities (to within a factor of 2) on both the first and second epoch plates. This filter is required to minimize the number of false detections from the often noisy/grainy photographic plates. The software does renormalize the intensities so that the total plate flux from all stars in the field are equal in the first and second epoch image. In principle, if all the stars in the field have the same color index, the renormalization will correct for it, and the stars will show the same (renormalized) flux on both images. However, if there are objects on the field that are bluer, or redder than the typical background star, their renormalized flux will be different on both images. The median value for the color of a field star is $B_J - R_F \approx 1.2$. In a typical field, where the red and blue plates have been renormalized by such that a $B_J - R_F = 1.2$ star yields similar instrumental flux values on both images, stars with $B_J - R_F < 0.4$ or with $B_J - R_F > 2.0$ will be missed by SUPERBLINK. In practice, this effect is mitigated by the fact that the photographic plate response is non-linear, but it remains true that unusually blue or red stars are likely to be missed by the code. In fact, close examination of some APMPM and SCR stars missed by SUPERBLINK shows that they are indeed quite red. Preliminary tests reveal that some tweaking of the SUPERBLINK software parameters, and relaxing of the automated rejection filters would increase the efficiency of the code, albeit at the expense of a larger number of false detections. These would then have to be filtered out by eye, requiring a larger investment of person-hours.

5. CONCLUSIONS

A search for high proper motion stars in the Digitized Sky Survey with the SUPERBLINK software has been completed

for an area of 8980 square degrees covering 87.1% of the sky south of $Decl. = -30^\circ$. A total of 1,147 stars with proper motion $\mu > 0.45'' \text{ yr}^{-1}$ were detected by SUPERBLINK, of which 182 are found to be new discoveries. Of these, there are 123 new stars with $\mu > 0.5'' \text{ yr}^{-1}$ (the canonical limit of the LHS catalog), including 5 stars with extremely large proper motions ($\mu > 1.0'' \text{ yr}^{-1}$). These make significant additions to the census of high proper motion stars at southern declinations.

A standard designation system is used to name the new high proper motion stars. It is based on the naming convention first introduced by Eggen (1979, 1980). At the time, the standard system was used by Eggen as a means to simplify the designation of some high proper motion stars which were then known under a variety of names. The original convention used $PMHHMMM \pm d d m m$, for a star with R1950 coordinates $R.A. = HH \text{ } MM.M$, $Decl. = \pm d d \text{ } m m$. Nowadays, there has been several new surveys and catalogs, each using its own prefix system, with much confusion resulting. We are again reaching a point where it is becoming desirable to uniformize the naming convention of the high proper motion stars. I propose a slight modification to the Eggen convention, in which the J2000 coordinates are used instead. High proper motion stars are thus to be designated according to the model $PM JHHMMM \pm d d m m$, for a star at the J2000 coordinates $R.A. = HH \text{ } MM.M$ $Decl. = \pm d d \text{ } m m$. I strongly encourage all researchers in the field to start following this convention as well, at least when naming a new discovery.

A reduced proper motion analysis suggests that 14 of the new high proper motion stars are white dwarfs, while 52 more are candidate halo subdwarfs. Most of the others are probably nearby red dwarfs. All these objects should be high priority targets for follow-up spectroscopy and astrometry (parallax measurements).

One notes that in the area covered by our survey, there are now 940 known $R_F > 10$ stars with $0.5 < \mu < 2.0'' \text{ yr}^{-1}$, where Luyten’s NLTT catalog listed 564. Much of the improvement comes from the fact that the SES blue and AAO red plates used in the SUPERBLINK survey are significantly deeper (20th magnitude) than the Bruce Proper Motion survey plates used by Luyten in the south, which had a limiting photographic magnitude $m_{pg} \approx 15.5$.

At southern declinations, the SUPERBLINK software has a detection rate of 80%–90% for stars with $10 < R_F < 19$, which falls short of matching the very high detection rates $\approx 99\%$ achieved in the northern sky survey. The main reason is that in the south, the DSS has only first epoch scans of blue (IIIaJ) plates, but second epoch scans of red (IIIaF) plates, while in the north, red plates were available for both the first and second epochs. The image subtraction techniques used by SUPERBLINK makes handling of blue/red pairs more problematic. Strategies to increase the SUPERBLINK detection rate of high proper motion stars in pairs of blue/red images are currently being considered and tested. In the meantime, the SUPERBLINK analysis of the remaining half of the southern sky ($0^\circ < Decl. < -30^\circ$) is now being performed, and new SUPERBLINK discoveries will be available soon.

Acknowledgments

The author gratefully acknowledges support from the Cordelia Corporation, from Hilary Lipsitz, and from the American Museum of Natural History.

This work has been made possible through the use of the

Digitized Sky Surveys. The Digitized Sky Surveys were produced at the Space Telescope Science Institute under U.S. Government grant NAG W-2166. The images of these surveys are based on photographic data obtained using the Oschin Schmidt Telescope on Palomar Mountain and the UK Schmidt Telescope. The plates were processed into the present compressed digital form with the permission of these institutions. The National Geographic Society - Palomar Observatory Sky Atlas (POSS-I) was made by the California Institute of Technology with grants from the National Geographic Society. The Second Palomar Observatory Sky Survey (POSS-II) was made by the California Institute of Technology with funds from the National Science Foundation, the National Geographic Society, the Sloan Foundation, the Samuel Oschin Foundation, and the Eastman Kodak Corporation. The Oschin Schmidt Telescope is operated by the California Institute of Technology and Palomar Observatory. The UK Schmidt Telescope was operated by the Royal Observatory Edinburgh, with funding from the UK Science and Engineering Research

Council (later the UK Particle Physics and Astronomy Research Council), until 1988 June, and thereafter by the Anglo-Australian Observatory. The blue plates of the southern Sky Atlas and its Equatorial Extension (together known as the SERC-J), as well as the Equatorial Red (ER), and the Second Epoch [red] Survey (SES) were all taken with the UK Schmidt.

This publication makes use of data products from the Two Micron All Sky Survey, which is a joint project of the University of Massachusetts and the Infrared Processing and Analysis Center/California Institute of Technology, funded by the National Aeronautics and Space Administration and the National Science Foundation.

The data mining required for this work has been made possible with the use of the SIMBAD astronomical database and VIZIER astronomical catalogs service, both maintained and operated by the Centre de Données Astronomiques de Strasbourg (<http://cdsweb.u-strasbg.fr>).

REFERENCES

- Cutri, R. M., *et al.* 2003, The 2MASS All-Sky Catalog of Point Sources University of Massachusetts and Infrared Processing and Analysis Center (IPAC/California Institute of Technology – *CDS-ViZier catalog number II/246*)
- Dawson, P. C. 1986, *ApJ*, 311, 984
- Eggen, O. J. 1979, *ApJS*, 39, 89
- Eggen, O. J. 1980, *ApJS*, 43, 457
- Hog E., Fabricius C., Makarov V.V., Urban S., Corbin T., Wycoff G., Bastian U., Schwekendiek P., & Wicenc A. 2000, The Tycho-2 Catalogue of the 2.5 Million Brightest Stars, *A&A*, 355, 27 (*CDS-ViZier catalog number I/259*)
- Gizis, J. E., & Reid, I. N. 1997, *PASP*, 109, 849
- Gliese, W., & Jahreiss, H. 1991, Preliminary Version of the Third Catalogue of Nearby Stars, *CDS-ViZier on-line Data Catalog: V/70A*.
- Lépine, S., Shara, M. M., & Rich, R. M. 2002, *AJ*, 124, 1190
- Lépine, S., Rich, R. M., & Shara, M. M. 2003, *AJ*, 125, 1598
- Lépine, S., Shara, M. M., & Rich, R. M. 2002, *AJ*, 126, 921
- Lépine, S., & Shara, M. M. 2005, *AJ*, in press
- Luyten W. J. 1979, LHS Catalogue: a catalogue of stars with proper motions exceeding 0.5" annually, University of Minnesota, Minneapolis (*CDS-ViZier catalog number I/87B*)
- Luyten W. J. 1979, New Luyten Catalogue of stars with proper motions larger than two tenths of an arcsecond (NLTT), University of Minnesota, Minneapolis (*CDS-ViZier catalog number I/98A*)
- Monet, D. G., *et al.* 2003, *AJ*, 125, 984, (The USNO-B1 catalog – *CDS-ViZier catalog number I/284*)
- Pokorny, R. S., Jones, H. R. A., & Hambly, N. C. 2003, *A&A*, 397, 584
- Reid, I. N., *et al.* 2003, *AJ*, 126, 3007
- Ruiz, M. T., Wischnjewsky, M., Rojo, P. M., & Gonzalez, L. E. 2001, *ApJS*, 133, 119
- Salim, S., & Gould, A. 2002, *ApJ*, 575, L83
- Salim, S., & Gould, A. 2003, *ApJ*, 582, 1011
- Scholz, R.-D., Irwin, M., Ibata, R., Jahreiss, H., & Malkov, O. Yu. 2000, *A&A*, 353, 958
- Subasavage, J. P., Henry, T. J., Hambly, N. C., Brown, M. A., & Jao, W.-C. 2005, *AJ*, in press
- Wroblewski, H., & Torres, A. 1997, *A&AS*, 122, 447
- Wroblewski, H., & Costa, E. 2001, *A&A*, 367, 725

FIG. A4.— Finding charts for the new high proper motion stars discovered with SUPERBLINK, as listed in Table 1.

FIG. A5.— Finding charts for the new high proper motion stars discovered with SUPERBLINK (continued).

FIG. A6.— Finding charts for the new high proper motion stars discovered with SUPERBLINK (continued).

APPENDIX FINDER CHARTS

Finder charts of high proper motion stars are generated as a by-product of the SUPERBLINK software. We present here finder charts for all the new, high proper motion stars presented in this paper and listed in Table 1. All the charts consist of pairs of $4.25' \times 4.25'$ images showing the local field at two different epochs. The name of the star is indicated in the center just below the chart, and corresponds to the name given in Table 1. To the left is the POSS-I field, with the epoch of the field noted in the lower left corner. To the right is the modified POSS-II field which has been shifted, rotated, and degraded in such a way that it matches the quality and aspect of the POSS-I image. The epoch of the POSS-II field is noted on the lower right corner. High proper motion stars are identified with circles centered on their positions at the epoch on the plate.

The charts are oriented in the local X-Y coordinate system of the POSS-I image; the POSS-II image has been remapped on the POSS-I grid. This means that north is generally up and east left, but the fields might appear rotated by a small angle for high declination objects. Sometimes a part of the field is missing: this is an artifact of the code. SUPERBLINK works on $17' \times 17'$ DSS subfields. If a high proper motion star is identified near the edge of that subfield, the output chart appears truncated.

FIG. A7.— Finding charts for the new high proper motion stars discovered with SUPERBLINK (continued).

FIG. A8.— Finding charts for the new high proper motion stars discovered with SUPERBLINK (continued).

FIG. A9.— Finding charts for the new high proper motion stars discovered with SUPERBLINK (continued).

FIG. A10.— Finding charts for the new high proper motion stars discovered with SUPERBLINK (continued).

FIG. A11.— Finding charts for the new high proper motion stars discovered with SUPERBLINK (continued).

FIG. A12.— Finding charts for the new high proper motion stars discovered with SUPERBLINK (continued).

TABLE A1
NEW HIGH PROPER MOTION STARS.

Star	$\alpha(J2000)$	$\delta(J2000)$	μ ($''$ yr $^{-1}$)	μ_{RA} ($''$ yr $^{-1}$)	μ_{Decl} ($''$ yr $^{-1}$)	Δt^a (yr)	μ_{err}^b ($''$ yr $^{-1}$)	B_J^c	R_F	I_N	J^d	H	K_s	class
PM J00151-5919	0 15 10.13	-59 19 56.7	0.483	0.473	0.097	16.02	0.020	19.6	17.0	13.5	12.14	11.56	11.21	d
PM J00168-7233	0 16 51.97	-72 33 46.4	0.507	-0.383	-0.332	9.92	0.032	19.0	17.0	14.8	13.33	12.84	12.57	d
PM J00294-6900	0 29 26.87	-69 00 13.3	0.486	0.465	-0.139	13.89	0.023	18.0	16.7	14.3	13.22	12.74	12.47	d
PM J00327-7641	0 32 43.62	-76 41 28.7	0.593	0.592	0.032	9.92	0.032	19.3	17.4	15.5	14.58	14.03	13.81	sd
PM J00344-6849	0 34 28.77	-68 49 29.7	0.508	-0.016	-0.508	13.89	0.023	19.5	18.8	17.8
PM J00522-6201	0 52 15.28	-62 01 54.6	1.073	1.065	0.122	15.09	0.021	19.7	16.7	13.3	12.15	11.74	11.37	d
PM J00568-7603	0 56 53.20	-76 03 43.8	0.457	0.194	-0.414	13.96	0.023	...	17.5	15.1	12.57	11.99	11.62	d
PM J01009-7904	1 00 56.07	-79 04 25.2	0.450	-0.270	-0.360	14.97	0.021	...	11.9	10.0	8.80	8.17	7.88	d
PM J01082-3714W	1 08 13.21	-37 14 39.2	0.509	-0.128	-0.492	17.39	0.018	...	15.2	13.2	12.84	12.36	12.12	sd
PM J01082-3714E	1 08 13.69	-37 14 39.1	0.509	-0.128	-0.492	17.39	0.018	...	15.2	14.1	13.41	12.97	12.70	sd
PM J01184-7504	1 18 29.66	-75 04 55.0	0.454	0.446	0.081	13.96	0.023	19.7	15.5	...	10.85	10.29	10.02	d
PM J01253-4545	1 25 18.02	-45 45 31.1	0.748	0.517	-0.541	13.82	0.023	18.0	16.9	18.7	15.11	14.84	14.91	wd
PM J01598-4736	1 59 48.21	-47 36 12.3	0.466	0.272	-0.378	13.05	0.025	...	16.2	15.1	13.80	13.30	13.04	sd
PM J03007-4653	3 00 45.15	-46 53 50.6	0.745	0.676	0.312	16.95	0.019	18.3	15.4	12.7	11.79	11.31	11.02	d
PM J03064-3325	3 06 26.46	-33 25 42.9	0.972	-0.164	-0.957	16.01	0.020	19.5	16.7	15.8	14.35	13.85	13.58	sd
PM J03116-3113	3 11 37.99	-31 13 21.2	0.544	0.162	-0.520	13.99	0.023	20.8	18.3	16.3	14.37	13.88	13.63	d
PM J03229-8159	3 22 59.54	-81 59 54.4	0.504	0.383	0.327	12.11	0.026	...	18.2	14.8	13.02	12.48	12.08	d
PM J03245-5220	3 24 32.99	-52 20 39.3	0.823	-0.444	-0.692	11.92	0.027	17.2	14.6	11.6	11.10	10.51	10.17	d
PM J03286-6756	3 28 38.30	-67 56 26.5	0.469	0.451	0.129	5.28	0.061	...	17.2	14.7	13.09	12.66	12.33	d
PM J03536-5006	3 53 36.57	-50 06 00.9	0.523	0.255	0.457	17.21	0.019	...	20.5	18.5
PM J04356-6105	4 35 37.39	-61 05 40.4	0.502	0.432	0.256	14.71	0.022	17.5	16.5	16.0	15.70	15.21	15.10	wd
PM J05175-4227	5 17 35.96	-42 27 54.4	0.452	0.191	-0.410	15.06	0.021	...	12.8	11.7	11.80	11.31	11.06	sd
PM J05472-6009	5 47 14.62	-60 09 50.5	0.475	0.164	-0.445	17.28	0.019	20.9	16.4	...	13.39	12.89	12.68	sd
PM J05597-4519	5 59 44.05	-45 19 10.5	0.819	0.449	0.685	12.87	0.025	18.7	16.8	15.4	14.15	13.61	13.41	sd
PM J06491-7603	6 49 06.65	-76 03 50.1	0.512	0.428	0.280	12.88	0.025	...	16.7	16.0	14.88	14.43	14.33	sd
PM J07096-3941	7 09 37.05	-39 41 52.0	0.472	-0.124	-0.455	14.86	0.022	16.7	14.7	12.5	11.77	11.21	10.99	d
PM J07096-4648	7 09 37.27	-46 48 59.1	0.456	0.137	0.434	14.81	0.022	...	14.0	13.1	12.20	11.70	11.49	sd
PM J07110-3824	7 11 00.96	-38 24 46.1	0.893	0.516	-0.728	14.06	0.023	20.6	15.6	13.0	11.09	10.55	10.23	d
PM J07185-3351	7 18 30.75	-33 51 24.5	0.461	-0.024	0.461	14.93	0.021	19.0	18.4	17.8
PM J07228-3042	7 22 51.34	-30 42 34.4	0.494	0.323	0.374	15.11	0.021	18.3	17.4	17.2	16.42	15.69	15.52	wd
PM J07253-3742	7 25 21.57	-37 42 59.1	0.587	0.211	-0.548	14.06	0.023	13.3	12.1	10.1	9.06	8.42	8.22	d
PM J07283-5812	7 28 23.20	-58 12 31.1	0.482	0.367	-0.312	14.83	0.022	...	12.9	12.4	11.60	10.97	10.84	sd
PM J07293-4804	7 29 21.66	-48 04 27.3	0.450	0.361	0.266	14.16	0.023	14.5	12.7	10.9	10.02	9.44	9.19	d
PM J07401-4257	7 40 11.83	-42 57 40.7	0.703	-0.436	0.551	14.00	0.023	15.5	12.5	10.3	8.68	8.09	7.77	d
PM J07433-5457	7 43 18.57	-54 57 30.0	0.484	-0.098	0.474	14.89	0.021	...	18.1	15.1	13.19	12.61	12.27	d
PM J07571-4021	7 57 07.87	-40 21 33.5	0.551	-0.532	0.143	12.20	0.026	17.3	14.5	15.7	11.41	10.92	10.65	d
PM J08152-3600	8 15 15.99	-36 00 59.5	0.639	-0.105	0.630	15.17	0.021	16.2	15.0	12.6	10.74	10.17	9.88	d
PM J08172-6808	8 17 16.66	-68 08 36.7	0.551	-0.301	0.461	14.06	0.023	18.9	16.8	15.5
PM J08186-3110	8 18 40.24	-31 10 19.6	0.817	0.224	-0.785	14.05	0.023	16.1	15.1	14.9	14.92	14.73	14.83	wd
PM J08276-3003	8 27 40.89	-30 03 00.0	0.594	-0.326	0.497	14.05	0.023	16.3	14.1	12.2	10.67	10.17	9.92	d
PM J08300-5039	8 30 00.78	-50 39 46.2	0.989	-0.568	0.810	14.11	0.023	15.7	13.8	12.5	10.70	10.15	9.90	d
PM J08355-3400	8 35 31.73	-34 00 36.9	0.546	-0.138	-0.529	12.26	0.026	16.0	14.3	11.2	9.90	9.37	9.08	d
PM J08446-4805	8 44 38.92	-48 05 21.8	0.748	-0.224	0.713	14.11	0.023	14.4	12.7	10.7	9.36	8.81	8.56	d
PM J08458-3051	8 45 51.96	-30 51 31.3	0.518	-0.477	-0.201	13.97	0.023	16.4	14.5	12.7	10.82	10.30	10.04	d
PM J08463-4407	8 46 20.99	-44 07 22.0	0.477	0.462	-0.117	15.17	0.021	17.5	16.3	14.8	12.80	12.26	12.04	d
PM J08471-3046	8 47 09.70	-30 46 12.0	0.528	0.062	-0.524	13.97	0.023	15.5	13.4	12.1	10.39	9.91	9.60	d
PM J08496-3138	8 49 38.94	-31 38 22.9	0.506	-0.174	0.475	13.97	0.023	16.4	14.8	13.2	11.69	11.16	10.91	d
PM J08503-5848	8 50 21.34	-58 48 06.7	0.612	-0.418	0.447	14.84	0.022	18.0	17.7	17.1	16.74	16.90	16.83	wd
PM J09047-3804	9 04 46.49	-38 04 07.0	0.614	0.408	-0.458	14.80	0.022	17.3	14.8	13.7	12.03	11.57	11.36	sd
PM J09172-3849	9 17 13.61	-38 49 36.0	0.494	-0.086	0.486	14.80	0.022	21.4	14.8	13.5	11.56	11.12	10.80	d
PM J09181-4437	9 18 08.62	-44 37 24.5	0.501	-0.405	0.295	13.98	0.023	17.3	16.8	16.5	15.59	15.37	14.89	wd
PM J09204-4922	9 20 26.02	-49 22 34.7	0.561	-0.406	0.387	14.81	0.022	17.8	15.9	12.7	11.33	10.82	10.53	d
PM J09233-3537	9 23 23.68	-35 37 58.3	0.485	-0.437	-0.210	14.03	0.023	16.8	13.8	12.9	12.24	11.72	11.53	sd
PM J09237-7248	9 23 42.50	-72 48 36.7	0.472	-0.360	0.305	14.88	0.022	...	15.1	13.6	12.63	12.07	11.82	sd

TABLE A1 — *Continued*

Star	α (J2000)	δ (J2000)	μ ($''$ yr $^{-1}$)	μ_{RA} ($''$ yr $^{-1}$)	μ_{Decl} ($''$ yr $^{-1}$)	Δt^a (yr)	μ_{err}^b ($''$ yr $^{-1}$)	B_J^c	R_F	I_N	J^d	H	K_s	class
PM J09271-4137	9 27 07.19	-41 37 12.0	0.476	0.389	-0.274	14.28	0.022	...	11.3	11.0	10.32	9.89	9.80	sd
PM J09376-3852	9 37 36.23	-38 52 23.0	0.586	-0.446	0.380	14.28	0.022	...	16.6	16.5	16.03	15.60	15.97	wd
PM J09396-6135	9 39 38.82	-61 35 11.3	0.481	0.467	0.112	14.81	0.022	19.1	13.2	...	10.80	10.30	9.98	d
PM J09566-4234	9 56 36.99	-42 34 27.3	0.658	0.382	-0.536	14.99	0.021	...	14.9	12.5	10.99	10.47	10.21	d
PM J09598-5027	9 59 53.94	-50 27 17.7	0.677	-0.665	0.128	15.83	0.020	16.4	15.6	15.6	15.46	15.20	14.82	wd
PM J10026-7519	10 02 37.66	-75 19 22.7	0.523	-0.371	0.368	14.95	0.021	...	16.9	14.6	12.60	11.98	11.67	d
PM J10050-4322	10 05 03.11	-43 22 28.2	0.632	-0.589	0.228	14.07	0.023	15.1	13.3	11.0	9.85	9.32	9.06	d
PM J10185-5254	10 18 30.01	-52 54 44.3	0.514	-0.297	0.419	19.10	0.017	16.4	13.8	13.3	13.74	13.29	13.04	wd
PM J10256-4703	10 25 39.40	-47 03 51.1	0.477	-0.445	0.170	14.07	0.023	19.9	17.5	16.2	15.05	14.63	14.23	sd
PM J10326-5255	10 32 40.69	-52 55 05.8	0.558	-0.512	0.221	19.10	0.017	...	15.8	...	11.98	11.38	11.01	d
PM J10346-4259	10 34 37.86	-42 59 57.0	0.471	-0.422	0.208	14.06	0.023	16.7	14.9	13.4	11.65	11.15	10.89	d
PM J10352-7424	10 35 12.32	-74 24 57.0	0.461	-0.397	0.233	14.95	0.021	...	15.8	...	13.40	12.84	12.58	sd
PM J10382-4933	10 38 15.18	-49 33 44.6	0.682	-0.333	-0.595	15.03	0.021	...	13.9	11.7	10.31	9.72	9.43	d
PM J10395-3820	10 39 32.40	-38 20 02.0	0.702	-0.196	-0.674	13.40	0.024	16.9	15.1	...	10.85	10.30	10.00	d
PM J10538-3858	10 53 49.42	-38 58 59.0	0.558	-0.347	0.436	18.10	0.018	15.7	14.1	12.4	10.91	10.43	10.13	d
PM J10587-3854	10 58 47.12	-38 54 14.8	0.622	-0.603	0.151	18.10	0.018	16.4	14.5	12.4	11.01	10.52	10.21	d
PM J11076-4105	11 07 40.05	-41 05 44.2	0.492	-0.475	0.129	14.90	0.021	22.3	18.1	16.0	14.28	13.80	13.51	d
PM J11094-4631	11 09 28.34	-46 31 10.0	0.452	-0.447	0.066	18.77	0.017	...	15.6	14.0	12.35	11.88	11.55	d
PM J11104-3608	11 10 29.04	-36 08 24.5	0.535	-0.531	-0.071	14.13	0.023	...	14.6	18.7	10.93	10.34	10.00	d
PM J11256-3834	11 25 37.31	-38 34 42.9	0.541	-0.528	-0.119	14.90	0.021	...	13.8	...	10.09	9.51	9.19	d
PM J11308-4120	11 30 48.27	-41 20 20.9	0.454	-0.441	-0.107	14.90	0.021	16.8	15.0	13.2	12.09	11.52	11.32	d
PM J11329-4039	11 32 57.95	-40 39 21.6	0.786	-0.685	0.385	19.14	0.017	15.7	13.5	11.5	10.38	9.89	9.65	d
PM J11413-3624	11 41 21.53	-36 24 34.7	0.590	0.532	0.255	15.93	0.020	...	12.4	10.1	8.49	7.97	7.70	d
PM J11480-4523	11 48 03.32	-45 23 01.8	0.635	-0.536	-0.340	14.12	0.023	16.9	14.2	13.8	14.89	14.76	14.60	wd
PM J11495-4248	11 49 31.69	-42 48 10.4	0.989	-0.979	-0.136	19.14	0.017	16.0	13.3	12.3	11.67	11.11	10.90	sd
PM J11511-4142	11 51 07.82	-41 42 17.3	0.600	-0.569	-0.189	19.14	0.017	...	15.3	12.8	11.51	10.99	10.68	d
PM J11578-5022	11 57 50.47	-50 22 32.1	0.478	-0.397	-0.265	14.85	0.022	...	12.4	10.8	9.27	8.65	8.37	d
PM J11596-4256	11 59 37.65	-42 56 39.1	0.603	-0.446	-0.405	17.65	0.018	15.4	12.3	10.6	9.54	8.98	8.72	d
PM J12042-4037	12 04 15.50	-40 37 52.1	0.603	0.230	-0.557	17.06	0.019	14.9	12.9	10.8	9.57	9.02	8.75	d
PM J12088-3723	12 08 51.03	-37 23 27.3	0.477	0.346	-0.329	15.86	0.020	16.0	14.3	12.0	10.62	10.08	9.78	d
PM J12146-4603	12 14 40.02	-46 03 14.2	0.797	-0.747	-0.276	17.65	0.018	16.9	14.6	12.3	10.32	9.75	9.44	d
PM J12159-5014	12 15 56.96	-50 14 19.3	0.665	-0.665	0.001	14.85	0.022	19.0	17.2	15.8	14.64	14.21	14.13	sd
PM J12201-4546	12 20 08.01	-45 46 18.3	0.750	-0.702	0.262	17.65	0.018	...	14.8	13.6	12.70	12.16	11.95	sd
PM J12225-4002	12 22 32.28	-40 02 12.2	0.602	-0.577	-0.170	17.06	0.019	19.8	17.5	14.5	12.60	11.98	11.62	d
PM J12277-4541	12 27 46.91	-45 41 17.1	1.321	-1.285	0.301	15.11	0.021	16.4	14.5	13.2	12.75	12.40	12.27	sd
PM J12300-3411	12 30 01.77	-34 11 23.9	0.563	-0.465	-0.317	15.92	0.020	15.3	13.6	11.2	9.34	8.77	8.44	d
PM J12313-4018	12 31 21.19	-40 18 36.8	0.569	-0.568	-0.023	13.02	0.025	16.2	14.0	12.1	10.44	9.94	9.64	d
PM J12346-5640	12 34 40.35	-56 40 12.4	0.559	-0.527	-0.183	14.65	0.022	19.8	16.8
PM J12355-4527	12 35 35.00	-45 27 03.8	0.450	-0.302	0.333	15.11	0.021	15.3	13.4	11.9	10.57	10.04	9.76	d
PM J12415-4717	12 41 33.18	-47 17 05.7	0.471	-0.454	-0.125	15.11	0.021	16.2	14.5	14.2	12.77	12.21	12.06	sd
PM J12472-4441	12 47 15.88	-44 41 50.0	0.688	-0.683	0.080	15.11	0.021	19.0	17.7	16.2	14.65	14.26	14.11	sd
PM J12515-3846	12 51 31.82	-38 46 12.5	0.625	-0.616	0.102	15.10	0.021	18.6	16.9	13.9	12.09	11.56	11.25	d
PM J13002-6024	13 00 15.78	-60 24 19.3	0.490	-0.437	0.221	15.02	0.021	16.9	15.4	12.9	11.76	11.21	10.84	d
PM J13077-7925	13 07 44.45	-79 25 10.3	0.514	-0.486	-0.165	17.10	0.019	...	17.8	17.3
PM J13084-3903	13 08 27.01	-39 03 32.0	0.456	-0.443	-0.110	15.10	0.021	...	16.9	14.1	12.60	12.07	11.78	d
PM J13095-3848	13 09 31.06	-38 48 04.4	0.572	-0.554	-0.141	15.10	0.021	...	12.8	10.9	9.86	9.30	9.05	d
PM J13139-5011	13 13 54.14	-50 11 09.6	0.468	-0.414	-0.216	15.04	0.021	18.9	16.3	13.7	12.38	11.83	11.50	d
PM J13276-3551	13 27 39.59	-35 51 01.0	0.518	-0.404	-0.325	15.94	0.020	16.8	14.7	12.3	11.13	10.60	10.33	d
PM J13338-5738	13 33 53.03	-57 38 42.5	0.710	-0.695	-0.144	17.93	0.018	19.1	17.2	15.0	12.84	12.32	12.03	d
PM J13379-4311	13 37 56.06	-43 11 30.1	0.522	-0.408	-0.325	16.03	0.020	17.1	15.3	13.5	11.70	11.11	10.79	d
PM J13384-3752	13 38 26.53	-37 52 50.4	1.265	-1.264	-0.031	15.94	0.020	...	15.5	13.2	11.75	11.28	10.97	d
PM J13423-3534	13 42 21.29	-35 34 50.8	0.903	-0.878	-0.211	15.94	0.020	19.0	16.5	...	13.76	13.22	12.94	sd
PM J13420-3544	13 42 00.21	-35 44 51.5	0.468	-0.454	0.113	15.94	0.020	18.8	16.3	...	13.31	12.80	12.52	sd
PM J13438-3447	13 43 48.93	-34 47 49.5	0.487	-0.479	-0.086	15.94	0.020	18.5	17.0	...	16.25	15.90	15.59	wd
PM J13548-4129	13 54 48.47	-41 29 04.8	0.690	-0.592	-0.354	14.70	0.022	19.4	18.1	16.8	15.52	15.06	14.63	sd

New high proper motion stars south of Decl. = -30°.

TABLE A1 — *Continued*

Star	α (J2000)	δ (J2000)	μ ($''$ yr $^{-1}$)	μ_{RA} ($''$ yr $^{-1}$)	μ_{Decl} ($''$ yr $^{-1}$)	Δt^a (yr)	μ_{err}^b ($''$ yr $^{-1}$)	B_J^c	R_F	I_N	J^d	H	K_s	class
PM J14005-3935	14 00 32.32	-39 35 29.3	0.508	-0.496	-0.109	14.70	0.022	17.0	15.8	14.1	13.47	12.90	12.66	sd
PM J14104-5001	14 10 29.10	-50 01 59.5	0.538	-0.158	-0.514	14.19	0.023	...	17.1	14.7	12.72	12.31	11.97	d
PM J14123-3941	14 12 21.16	-39 41 33.4	0.613	-0.538	-0.293	16.14	0.020	16.3	14.3	12.3	10.99	10.43	10.18	d
PM J14129-4001	14 12 58.26	-40 01 21.7	0.450	-0.414	-0.176	16.14	0.020	20.8	18.1	17.8
PM J14330-3846	14 33 03.36	-38 46 59.5	0.475	-0.465	-0.095	16.14	0.020	18.6	16.0	15.3	14.37	13.78	13.59	sd
PM J14344-4700	14 34 27.25	-47 00 15.6	0.517	-0.517	-0.002	18.09	0.018	21.1	15.2	...	11.94	11.47	11.20	d
PM J14373-4002	14 37 21.44	-40 02 49.1	0.509	-0.408	-0.304	13.80	0.023	15.9	14.3	12.4	10.79	10.21	9.90	d
PM J14382-6231	14 38 13.58	-62 31 39.5	0.695	-0.546	-0.429	17.34	0.018	...	13.4	12.8	10.52	9.98	9.72	d
PM J14435-5430	14 43 35.13	-54 30 44.6	0.645	-0.631	-0.131	15.19	0.021	18.0	15.8	13.9	11.96	11.41	11.14	d
PM J14441-3426	14 44 06.57	-34 26 46.5	0.493	-0.030	-0.492	13.98	0.023	...	13.7	11.0	9.74	9.18	8.88	d
PM J14440-4414	14 44 01.97	-44 14 40.8	0.509	-0.441	-0.254	18.09	0.018	20.5	17.0	15.1	13.33	12.81	12.50	d
PM J14500-3742	14 50 02.87	-37 42 09.6	0.511	-0.297	-0.416	13.80	0.023	15.0	13.3	11.0	9.95	9.37	9.07	d
PM J14558-3914	14 55 51.61	-39 14 33.1	0.786	-0.780	-0.095	13.80	0.023	20.7	14.7	...	12.50	11.98	11.79	sd
PM J14570-4705	14 57 05.32	-47 05 25.8	0.548	-0.411	-0.362	10.34	0.031	16.7	15.2	14.5	13.53	12.96	12.82	sd
PM J14570-5943	14 57 02.97	-59 43 46.8	0.617	-0.407	-0.463	17.34	0.018	17.9	15.7	13.9	12.48	12.01	11.78	d
PM J14585-5916	14 58 31.22	-59 16 42.3	0.472	-0.423	-0.210	18.02	0.018	...	13.8	...	10.48	9.85	9.58	d
PM J14596-4043	14 59 40.72	-40 43 19.6	0.754	-0.687	-0.308	13.87	0.023	17.9	16.6	14.5	14.29	13.80	13.47	sd
PM J15044-4353	15 04 29.26	-43 53 43.8	0.478	-0.414	-0.240	10.34	0.031	16.8	15.4	13.1	11.79	11.18	10.88	d
PM J15054-4620	15 05 27.37	-46 20 16.1	0.530	-0.462	-0.259	10.34	0.031	16.0	14.5	...	11.07	10.51	10.28	d
PM J15116-3403	15 11 38.66	-34 03 15.8	0.567	-0.165	-0.543	16.25	0.020	15.7	13.7	11.3	10.05	9.42	9.13	d
PM J15128-4354	15 12 52.34	-43 54 12.4	0.474	-0.244	-0.407	10.34	0.031	16.2	13.6	11.5	10.57	9.96	9.75	d
PM J15145-4625	15 14 31.88	-46 25 55.3	0.539	-0.538	-0.005	17.38	0.018	15.6	14.9	14.4	14.71	14.61	14.65	wd
PM J15184-3544	15 18 29.68	-35 44 11.2	0.481	-0.067	-0.477	16.25	0.020	...	15.8	14.5	13.73	13.28	13.10	sd
PM J15206-7137	15 20 41.70	-71 37 08.3	0.478	-0.396	-0.267	16.33	0.020	18.0	16.8	...	13.25	12.75	12.46	d
PM J15231-7711	15 23 11.17	-77 11 23.5	0.831	-0.772	-0.305	17.98	0.018	...	15.8	14.7	13.76	13.27	13.03	sd
PM J15246-6239	15 24 40.53	-62 39 27.1	0.497	-0.394	-0.303	17.06	0.019	...	13.9	12.4	10.93	10.48	10.18	d
PM J15252-4549	15 25 15.12	-45 49 36.5	0.457	-0.202	-0.410	17.38	0.018	18.4	16.4	15.3	14.49	14.02	13.76	sd
PM J15292-5620	15 29 15.30	-56 20 40.6	0.598	-0.576	-0.158	17.04	0.019	17.8	15.6	14.5	13.23	12.73	12.48	sd
PM J15322-3622	15 32 13.92	-36 22 30.7	0.462	-0.372	-0.274	15.85	0.020	...	13.0	...	10.10	9.54	9.28	d
PM J15334-3634	15 33 27.72	-36 34 02.4	0.552	-0.453	-0.316	15.85	0.020	16.4	14.2	12.5	11.54	10.99	10.76	d
PM J15345-6452	15 34 31.45	-64 52 54.8	0.455	-0.139	-0.434	17.06	0.019	15.9	14.1	12.4	11.19	10.65	10.39	d
PM J15413-3609	15 41 19.05	-36 09 10.8	0.529	-0.520	-0.094	15.85	0.020	17.6	16.1	13.5	11.97	11.45	11.11	d
PM J15547-3856	15 54 46.12	-38 56 17.4	0.454	-0.203	-0.406	17.82	0.018	16.2	13.6	11.8	11.19	10.69	10.46	d
PM J16006-3234	16 00 39.59	-32 34 11.4	0.534	-0.443	-0.298	14.22	0.023	20.2	17.3	15.9	14.43	14.04	13.69	sd
PM J16019-3421	16 01 55.61	-34 21 56.4	0.672	0.586	-0.328	14.22	0.023	...	15.0	12.5	10.96	10.33	9.98	d
PM J16087-4442	16 08 43.95	-44 42 28.3	0.596	-0.142	-0.579	17.89	0.018	20.2	14.3	...	10.88	10.35	10.10	d
PM J16138-3040	16 13 53.61	-30 40 57.9	0.457	-0.304	-0.341	14.72	0.022	16.5	15.1	13.5	13.15	12.58	12.38	sd
PM J16141-4044	16 14 07.03	-40 44 15.0	0.523	-0.433	-0.292	17.82	0.018	16.8	14.5	13.1	12.33	11.87	11.61	sd
PM J16169-4352	16 16 58.36	-43 52 17.1	0.496	-0.486	-0.099	16.84	0.019	17.5	15.6	13.9	12.28	11.78	11.48	d
PM J16256-6712	16 25 38.95	-67 12 21.4	0.698	-0.561	-0.415	14.08	0.023	18.1	16.8	14.3	12.45	11.95	11.60	d
PM J16364-8737	16 36 26.10	-87 37 06.2	0.451	-0.309	-0.328	18.67	0.017	17.8	17.2	17.4	16.59	16.26	16.75	wd
PM J16492-5142	16 49 13.81	-51 42 52.2	0.452	-0.262	-0.369	16.31	0.020	15.4	14.4	11.9	12.12	11.63	11.44	sd
PM J17037-6823	17 03 46.81	-68 23 29.3	0.503	-0.347	-0.363	15.02	0.021	16.8	14.6	13.1	13.13	12.65	12.47	sd
PM J17056-8608	17 05 38.35	-86 08 44.1	0.512	-0.305	-0.411	18.67	0.017	19.2	16.9	13.6	12.82	12.28	11.96	d
PM J17397-6322	17 39 46.10	-63 22 07.1	0.547	-0.098	-0.538	17.07	0.019	...	13.3	11.8	11.08	10.50	10.25	d
PM J18004-6358	18 00 29.82	-63 58 21.4	0.472	-0.183	-0.435	17.07	0.019	18.4	16.1	14.8	14.40	13.94	13.72	sd
PM J18036-6340	18 03 37.17	-63 40 47.9	0.484	-0.256	-0.411	17.27	0.019	17.2	15.5	14.3	13.67	13.13	12.92	sd
PM J18217-6101	18 21 46.25	-61 01 54.5	0.559	0.074	-0.554	19.99	0.016	20.3	18.1	14.6	12.82	12.29	11.96	d
PM J18286-4531	18 28 38.23	-45 31 08.1	0.501	-0.331	-0.376	15.92	0.020	19.0	14.7	15.3	12.24	11.72	11.43	sd
PM J18298-5131	18 29 51.30	-51 31 31.7	0.577	-0.241	-0.524	15.04	0.021	19.5	18.0	...	15.63	14.95	14.79	sd
PM J19105-4132	19 10 33.60	-41 32 50.6	0.676	0.125	-0.664	14.95	0.021	11.14	10.55	10.24	d
PM J19105-4133	19 10 34.60	-41 33 44.4	0.676	0.125	-0.664	14.95	0.021	...	13.0	11.0	9.85	9.24	9.03	d
PM J19103-4338	19 10 23.58	-43 38 37.2	0.450	-0.004	-0.450	14.74	0.022	...	15.7	13.7	11.86	11.28	10.99	d
PM J19110-3820	19 11 00.24	-38 20 31.9	0.585	0.547	-0.205	14.95	0.021	...	16.9	...	15.99	15.79	15.62	wd
PM J19167-3638	19 16 46.58	-36 38 04.1	1.340	-0.162	-1.329	15.04	0.021	18.1	15.8	14.9	13.66	13.12	12.95	sd

TABLE A1 — *Continued*

Star	$\alpha(J2000)$	$\delta(J2000)$	μ ($''$ yr $^{-1}$)	μ_{RA} ($''$ yr $^{-1}$)	μ_{Decl} ($''$ yr $^{-1}$)	Δt^a (yr)	μ_{err}^b ($''$ yr $^{-1}$)	B_J^c	R_F	I_N	J^d	H	K_s	class
PM J19184-4554	19 18 29.44	-45 54 30.8	0.616	-0.414	-0.456	14.74	0.022	...	15.1	13.1	11.21	10.65	10.30	d
PM J19248-3356	19 24 48.28	-33 56 09.7	0.574	0.319	-0.477	15.04	0.021	16.0	13.7	12.8	12.45	11.99	11.77	sd
PM J19261-4310	19 26 08.60	-43 10 56.4	1.142	-0.142	-1.133	16.96	0.019	...	15.8	13.7	11.94	11.42	11.12	d
PM J19285-3634	19 28 33.61	-36 34 30.3	0.503	0.024	-0.503	14.72	0.022	...	14.2	12.4	10.61	10.06	9.81	d
PM J19280-6028	19 28 00.48	-60 28 52.4	0.460	0.068	-0.455	13.77	0.023	...	16.6	14.5	13.97	13.41	13.23	sd
PM J19403-3944	19 40 21.30	-39 44 10.0	0.529	0.156	-0.505	14.20	0.023	...	13.8	17.4	10.38	9.84	9.57	d
PM J20444-4123	20 44 27.89	-41 23 51.6	0.505	0.357	-0.356	15.25	0.021	...	14.3	12.4	11.75	11.16	10.99	d
PM J20460-5458	20 46 01.48	-54 58 06.7	0.461	0.134	-0.441	15.04	0.021	...	18.5	16.7	15.29	14.80	14.41	sd
PM J20530-5409	20 53 03.90	-54 09 37.5	0.633	0.177	-0.608	15.04	0.021	18.7	16.6	13.8	12.17	11.66	11.35	d
PM J21324-3922	21 32 29.67	-39 22 50.1	0.513	0.447	-0.252	16.08	0.020	...	15.8	13.4	12.21	11.70	11.35	d
PM J22040-3347	22 04 02.27	-33 47 38.3	0.948	0.472	-0.822	14.14	0.023	...	14.5	...	12.32	11.81	11.60	sd
PM J22178-7753	22 17 53.89	-77 53 36.0	0.584	0.315	-0.492	15.92	0.020	18.9	17.0	15.5	14.53	14.07	13.91	sd
PM J22209-3346	22 20 57.91	-33 46 57.9	0.559	-0.102	-0.550	15.12	0.021	19.8	17.8	18.1
PM J22359-7722	22 35 57.74	-77 22 16.8	0.601	-0.224	-0.558	15.92	0.020	18.4	16.3	15.3	14.17	13.67	13.46	sd
PM J22387-6232	22 38 47.28	-62 32 22.7	0.504	0.305	-0.401	18.11	0.018	20.3	17.4	18.2
PM J22403-4931E	22 40 18.96	-49 31 01.4	0.504	0.457	0.212	14.87	0.022	15.1	13.3	10.7	9.93	9.38	9.03	d
PM J22403-4931W	22 40 18.67	-49 31 04.6	0.504	0.457	0.212	14.87	0.022	9.84	9.26	9.01	d
PM J23350-4904	23 35 04.31	-49 04 54.3	0.611	0.334	-0.511	17.33	0.018	...	15.5	13.9	13.29	12.75	12.52 sd	

^a Temporal baseline between the first and second DSS epoch.

^b Estimated proper motion error.

^c Photographic B_J (IIIaJ), R_F (IIIaF) and I_N (IVN) magnitudes from the USNO-B1.0 catalog.

^d Infrared JHK_s magnitudes from the 2MASS All-Sky Point Source Catalog.

This figure "f4.jpg" is available in "jpg" format from:

<http://arxiv.org/ps/astro-ph/0501266v2>

This figure "f5.jpg" is available in "jpg" format from:

<http://arxiv.org/ps/astro-ph/0501266v2>

This figure "f6.jpg" is available in "jpg" format from:

<http://arxiv.org/ps/astro-ph/0501266v2>

This figure "f7.jpg" is available in "jpg" format from:

<http://arxiv.org/ps/astro-ph/0501266v2>

This figure "f8.jpg" is available in "jpg" format from:

<http://arxiv.org/ps/astro-ph/0501266v2>

This figure "f9.jpg" is available in "jpg" format from:

<http://arxiv.org/ps/astro-ph/0501266v2>

This figure "f10.jpg" is available in "jpg" format from:

<http://arxiv.org/ps/astro-ph/0501266v2>

This figure "f11.jpg" is available in "jpg" format from:

<http://arxiv.org/ps/astro-ph/0501266v2>

This figure "f12.jpg" is available in "jpg" format from:

<http://arxiv.org/ps/astro-ph/0501266v2>